Renewable Energy xxx (xxxx) xxx-xxx

Contents lists available at ScienceDirect

Renewable Energy

journal homepage: www.elsevier.com

ELSEVIER

Maximizing energy production from hydropower dams using short-term weather forecasts

Shahryar Khalique Ahmad , Faisal Hossain *

Dept. of Civil and Environmental Engineering, Univ. of Washington, More Hall 201, Seattle, WA, 98195, USA

ARTICLE INFO

Article history:
Received 4 October 2018
Received in revised form 16 April 2019
Accepted 27 July 2019
Available online xxx

Keywords:
Hydropower
Maximization
Short-term weather forecasts
Reservoir operations optimization
Flood control

ABSTRACT

This study explores the maximization of hydropower generation by optimizing reservoir operations based on short-term inflow forecasts derived from publicly available numerical weather prediction (NWP) models. Forecast fields from the NWP model of Global Forecast System (GFS) were used to force the Variable Infiltration Capacity (VIC) hydrologic model to forecast reservoir inflow for 1–16 days lead time. The optimization of reservoir operations was performed based on the forecast of inflow. The concept was demonstrated for two dams in the United States. Results showed that a significantly greater amount additional hydroelectric energy benefit can be derived consistently than the traditional operations without optimization and weather forecasts. Goals of flood control and dam safety were also not compromised when exploring opportunities for hydropower maximization. An alternate data-based technique was also demonstrated to improve the forecasting skill and efficiency. The study clearly underscores the additional value of weather forecasts that are available publicly and globally from NWP models for any dam location for hydropower maximization. Given the on-going effort to coordinate strategies for sustainable energy production from renewable energy sources, it is timely that this concept be expanded further to current hydropower dam sites around the world.

1. Introduction

Improving production from renewable energy sources is required in reducing the dependence on fossil fuels and addressing the global energy security in a sustainable way. As envisioned by Ref. [1], unless a replacement energy infrastructure is developed well ahead of time, economic, social and political instability may ensue due to heavy fluctuation in the supplies and price of fossil fuel [2]. The renewable sources of energy are not subject to such price fluctuations as they come from the available natural sources of water, sunlight, wind, tides etc. [3]. A recent study concluded that the use of wind, solar, hydroelectric, tidal and geothermal energy is the most beneficial, among several other alternatives, for addressing pollution, public health, global warming, and energy security [4].

The use of wind, water and sunlight to suffice for the electricity demands within U.S. as well as worldwide has been explored by Refs. [1,5–7]. Some of these studies have projected the future renewable energy potential to lie exclusively in the variable sources of wind and solar power and claimed them to be sufficient to meet the energy demand [8–11]. However, hydropower remains a stable renewable source to generate the baseload power (minimum power needed at a steady rate) due to its relatively high capacity factor [12,77] and minimal potential interruptions to the system [13,14]. Factors that further necessitate studying hydropower systems include its significant operational flexibility with ability to store energy [15], instant power generation [16], low operating and maintenance costs [13], and capability of integration with intermittent renewables [15,17,18]. This is manifested in recent effort of wind-hydro combination projects by the German firm *Max Bögl* [19].

Within the U.S., over the past 65 years (1950–2015), hydropower has contributed 10% to the total and 85% to the renewable power generation [19]. However, the installation of newer hydropower capacity has declined in the past couple of decades. According to the U.S. Department of Energy [19], the amount of nation's net electricity generation contributed by hydropower has decreased, from 30% in 1950 to 7% in 2013, as nuclear power, coal, natural gas, and other sources were added to the nation's energy portfolio to meet rising demands. In the last decade, no large-scale hydropower dam project, exceeding 500 MW (MW), has been constructed in the U.S. due to factors such as lower economic growth, concerns related to environmental impacts, stagnant energy market, and uncertainties owing to the recent breakthroughs in the shale gas and oil industries [20]. Fig. 1 illustrates this stagnation observed in the growth of hydropower capacity after 1990. Further, as most economical hydropower sites in U.S. have already been explored over the previous century, any rise in the hydropower infrastructure is hardly expected [21]. Miniature hydropower and pump storage plants have recently appeared as alternatives using highly flexible pump as turbines (PAT) for utilization of hydropower without causing major human rehabilitation [77–79]. However, given that large-scale development of new hydropower dams has stagnated in the developed world such as the U.S., it is worthwhile to explore how existing infrastructure can be maximized

* Corresponding author.
Email address: fhossain@uw.edu (F. Hossain)

https://doi.org/10.1016/j.renene.2019.07.126
0960-1481/

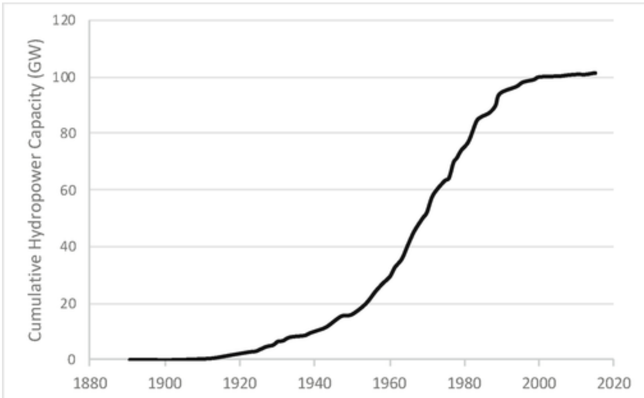

Fig. 1. Cumulative installed hydropower capacity from 1890 to 2015 over the United States (Reproduced from Ref. [2]).

of its operational effectiveness to provide more power to the energy grid by optimizing the operations [22].

The current management of most federally-operated reservoirs in the U.S. is based on rule curves that outline the reservoir storage targets to be met at specific time intervals of the year. The rule curves were designed based on existing storage volumes using a climatology of historical flow observations [23,24]. Operating strictly based on these rules, without considering the altered demands or changes in inflow patterns [71,72] can cause mishandling of an impending and unexpected reservoir inflow situation at the weather scale. Such a situation can lead to missed hydroelectric energy [20]. For example, in a weaker-than-average month of the flood season, lowering the pool to rule curve level too early can result in significant loss in power generation, which could be avoided if the inflow forecasts are made ahead of time. Thus, it is timely to leverage the advancements in atmospheric modeling for forecasting the weather [25] and optimization techniques to achieve the goal of maximizing hydropower energy and realize more efficient and 'smart' reservoir operations management.

The numerical weather prediction (NWP) weather models from various meteorological agencies produce weather scale forecasts fields of precipitation, temperatures, wind speed, soil moisture etc. in three dimensions over the entire globe. These publicly available forecasts represent an underutilized low-hanging fruit for the hydropower community. Currently, the integration of such forecasts into existing water management decision processes at weather scale is not yet popular or mainstream due to the traditional risk averse nature of water managers. The major concerns include low forecast skill and mismatch in the scales of forecasts from those required by the stakeholders [13,22,26,27]. However, a recent study concluded that the forecast skill of NWP models at a lead time of 7 days has improved from 50% in 1995 to more than 70% in 2015 [15]. Such an improvement can capture the peaks of a flood event and can be utilized to adjust the dam operations accordingly.

Reservoirs in the snow-dominated regions like the west coast (e.g. Columbia River basin) frequently use seasonal projections of climate, snowpack forecast etc. to optimize their operations [13,27]. Ongoing projects such as Integrated Forecast and Reservoir Management (INFORM) [28] and Forecast Informed Reservoir Operations [29], that have focused over specific watersheds, are also utilizing short-term weather forecasts for operating the reservoirs. Another issue is the coarse resolution of the NWP forecast fields that are often not detailed enough to be applied over the relatively small reservoir catchments. To address this scale limitation, dynamic downscaling technique can be used to resolve the atmospheric processes at finer spatial scales [30–32]. To the best of our knowledge, there has not been any study to explore the value of dynamically downscaled NWP based-forecasts specifically for hydropower maximization.

To utilize the forecast inflow information for generating more energy, the reservoir system needs an optimal and more informed set of release decisions updated dynamically based on the current reservoir state and future inflow. Various optimization techniques have been proposed in the past, and an extensive literature review and evaluation of different state-of-the-art approaches can be found in Refs. [21,33–35]. The optimization objective is the key as there are a plenty of studies focusing on single user benefits. These include optimizations for hydropower production [36–38], flood control and security [23,39,40], water supply [41,42], irrigation and crop planning [43,44] and environmental concerns [20]. However, due to the wide-ranging diversity of property rights and stakeholders, optimizing for a single stakeholder is ill-advised, rather the competing purposes (such as flood control and irrigation) needs to be balanced for extracting equitable benefits out of the existing infrastructure.

In several multi-objective optimization studies [45–52], the focus has been on the dams with significantly large reservoir storage capacity. The value of weekly streamflow forecasts was evaluated by Ref. [80] over three different reservoir systems. Wasimi and Kitanidis [81] analyzed the daily forecasts specifically to minimize flood damage from multi-reservoir system operations during floods. Short-term forecasts, as used here, are likely more valuable for the dams with reservoir capacity smaller than the annual inflow volume [27]. This study specifically explores such dams, usually unexplored in existing literature, for hydropower operations based on weather-scale forecasts while maintaining flood control and dam safety. Further, as underscored by Ref. [82], the uncertainty of hydrologic forecasts must be considered to avoid fatal decisions. A scheme for obtaining probabilistic inflow forecasts based on ensemble NWP fields is also described in this study.

The key novel elements that distinguish this study from the existing literature include: (a) demonstration of the value of publicly available, dynamically downscaled NWP-based forecasts, to obtain reservoir inflow forecasts; (b) derivation of probabilistic forecasts using NWP forecast fields; (c) focusing on small-medium storage dams that receive unregulated inflow; (d) coupling of the forecasts with reservoir optimization for hydropower maximization without compromising downstream flood safety. Most of the published literature, to the best of our knowledge, focusses on flood control or hydropower but never together despite the obvious and competing constraints each pose on reservoir operations.

The overarching research question addressed is – *can short-term weather forecasts from numerical weather prediction improve the hydroelectric energy production for small and medium storage dams without compromising flood security, dam safety and environmental flow constraints?* Hereafter 'short-term' is used to refer to a period of up to 16 days (forecast horizon of the NWP model). A schematic of the approach highlighting the major components of the study is shown in Fig. 2 and is explained in the following sections.

2. Material and methods

2.1. Study region and data

An exploration was made for dams satisfying the following criteria: (i) operated for hydropower generation or flood control as their primary or secondary purpose, (ii) have reservoir storage capacity less than a threshold of 1,700 kaf (2.1 km^3) (98th percentile value for reservoir storage within U.S., see Fig. 3), (iii) located upstream in the dam network (in case of a multi-reservoir system) to receive unregu-

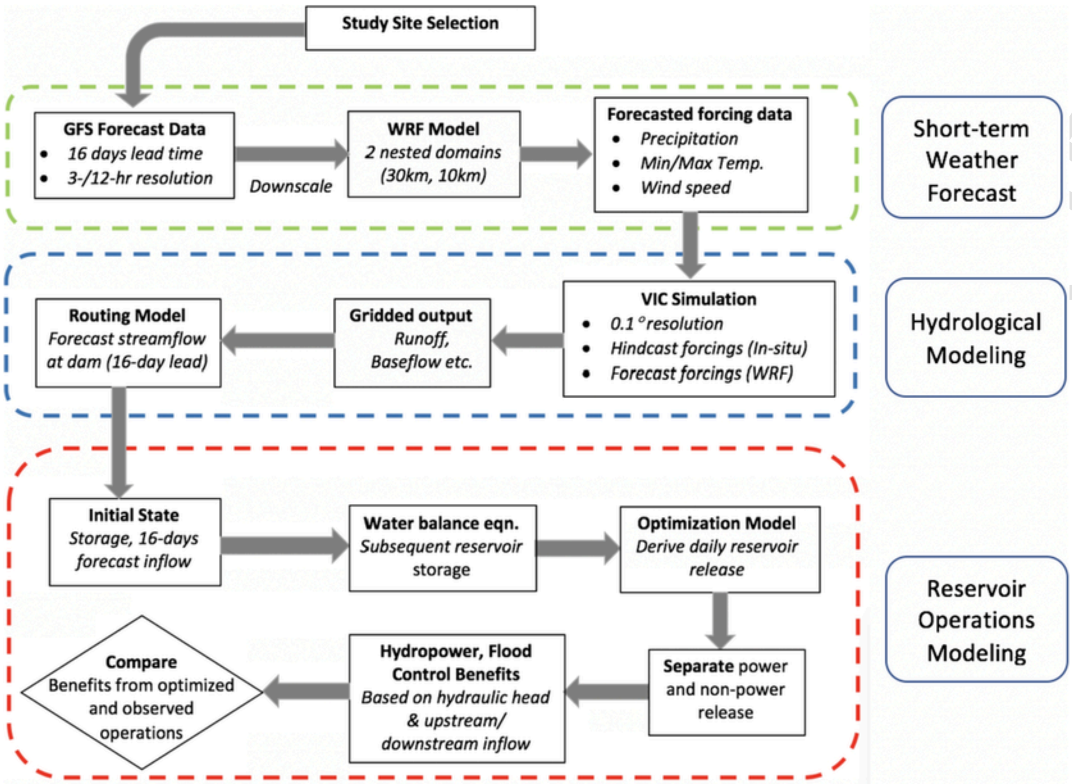

Fig. 2. Illustration of the approach used in this study. Green box – forecasting; Blue box – hydrologic modeling; Red box – optimization component. VIC is the hydrologic model for predicting inflows. GFS is NOAA's Global Forecasting System for weather forecasts.

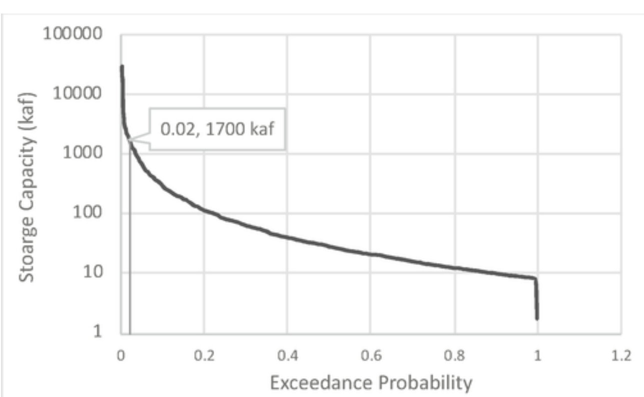

Fig. 3. Distribution of the storage capacity of dams in U.S. Data obtained from Global Reservoir and Dam (GRanD) database [73].

lated inflow, to facilitate hydrological modeling, and (iv) reservoir storage capacity smaller than annual inflow volume for the short-term forecasts to be valuable [27]. Out of several potential locations, Detroit dam in Oregon and Pensacola dam in Oklahoma, were selected based on the data availability and processing time constraints. Both the Detroit dam, located at the North Santiam River forming Detroit Lake, and Pensacola dam on the Neosho River forming Grand Lake are primarily used for hydropower and flood control. The powerhouse at Detroit dam contains two Francis turbine units with a combined nameplate capacity of 100MW, while Pensacola dam, Oklahoma's first hydroelectric power plant, consists of six turbine generator units with the nameplate capacity of 120MW. The observed streamflow data was obtained from the U.S. Army Corps of Engineers (USACE) [53,54]. The reservoir storage capacity and ratio with annual inflows are shown in Table 1 and locations of the selected dams in Fig. 4.

2.2. Short-term NWP based forecasts

Real-time short-term (1–16 days) forecast data from the Global Forecast System (GFS) global-scale NWP model was acquired at 0.5° resolution. The global forecasts are produced four times a day for 1–16 days lead time in almost real-time by National Centers for Environmental Prediction (NCEP) [76]. Dynamic downscaling was performed using the numerical Weather Research Forecasting (WRF) model to output forecasts at 0.1° resolution. WRF, a mesoscale atmospheric numerical modeling system, has demonstrated its capability for constructing the atmospheric conditions, at both local and regional scales [55,56]. Two nested domains of 10 km and 30 km were used for both the dams as shown in Fig. 5.

In a numerical model like WRF, the Microphysics (MP) and Cumulus Parameterization (CP) schemes are the controlling factors for precipitation as reported in existing literature [55,57]. As the Detroit dam lies in the Pacific Northwest region, the model configurations were inherited from the forecast model runs of Department of Atmos-

Table 1
Comparison of Storage Capacity and Annual Inflow for the two dams.

Dam	Drainage Basin Area (km^2)	Storage Capacity (km^3)	Annual Inflow (km^3)	Capacity-Annual Inflow Ratio
Detroit	1435.4	0.56	1.75	0.32
Pensacola	26847.9	2.06	7.40	0.28

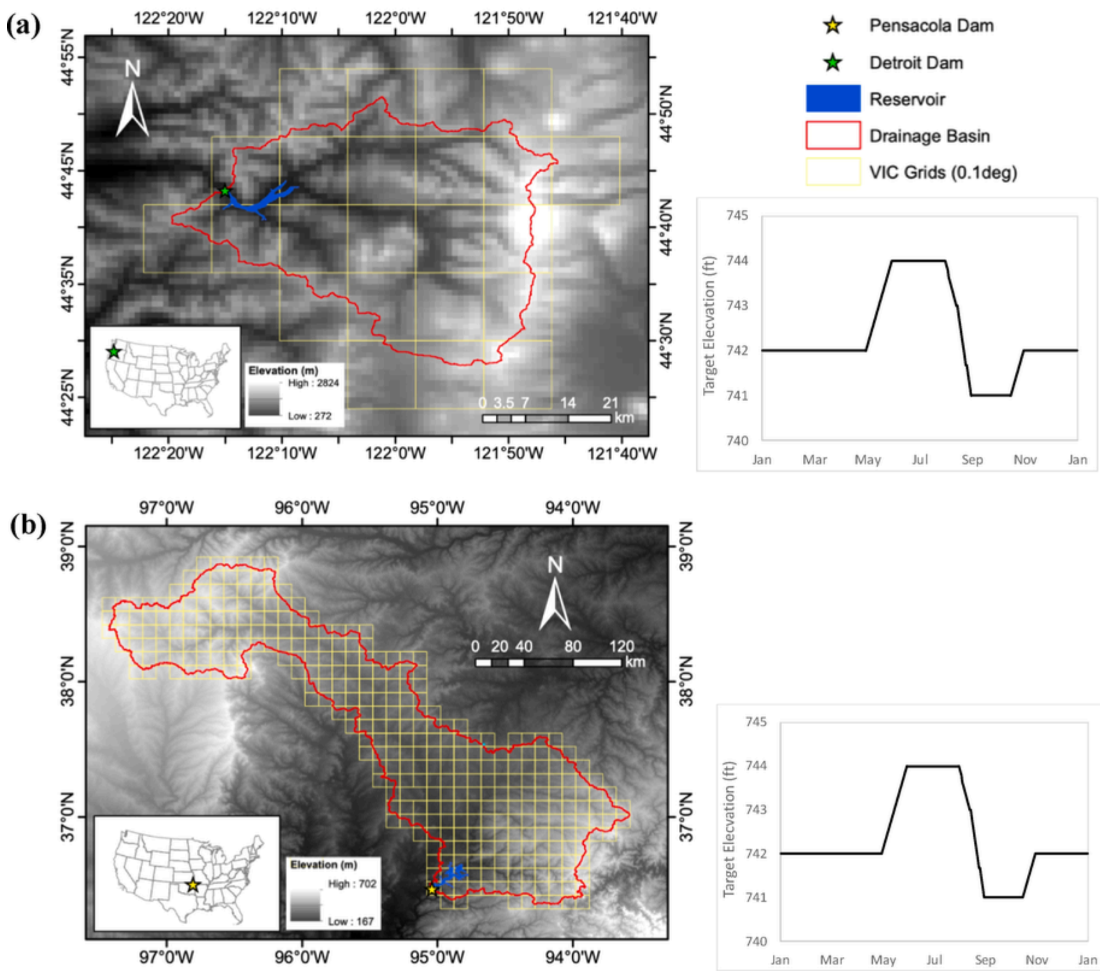

Fig. 4. Location, drainage boundaries, VIC model grids (0.1°) on the left panel and rule curves for (a) Detroit Dam, OR; (b) Pensacola Dam, OK, on the right panel (1 ft = 0.305m).

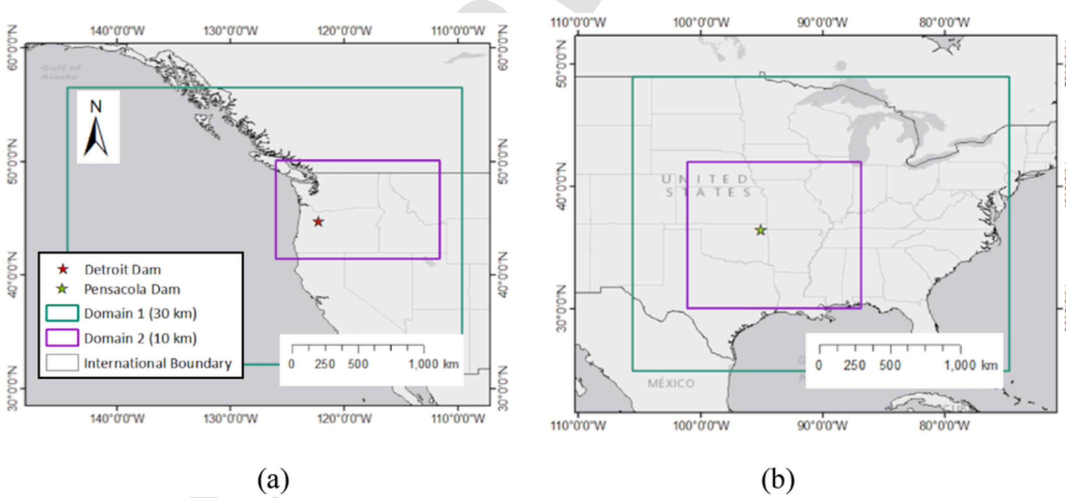

Fig. 5. The nested domains for WRF simulation at 30 km and 10 km, for (a) Detroit Dam, OR and (b) Pensacola Dam, OK.

pheric Sciences at the University of Washington [58]. The Thompson graupel scheme was considered for MP and Grell-Devenyi ensemble scheme for CP. For Pensacola dam, the Morrison microphysics scheme was used as recommended by Ref. [55] for extreme storm simulations. Appendix A evaluates the performance of WRF setup for both the dams.

2.3. Hydrologic model

The macroscale semi-distributed Variable Infiltration Capacity (VIC) hydrologic model [59,60] was chosen to model the reservoir inflow. The VIC model is forced with the time series of gridded precipitation, minimum and maximum temperature, and wind speed. The macroscale model was run at a daily time scale at 0.1° spatial resolution to ensure that the basin contains enough grid cells for simulation. The hindcast forcings were obtained from NCDC Global Surface Summary of the Day data [61] while the WRF-downscaled GFS fields provided the forecast forcings for the VIC model. To obtain the inflow at the downstream station of basin, routing of streamflow was performed separately using the routing model of Lohmann et al. [62,63]. Model calibration was performed by adjusting the parameters of VIC model that govern baseflow recession, infiltration, and soil layer depths to match the simulated streamflow with reference data, minimizing the root mean squared error (RMSE). The calibration and validation details of VIC model are provided in Appendix B.

2.4. Reservoir operations model

The next step (Fig. 2, red box) is to model the reservoir operations using the forecast inflow information by optimizing the releases from the reservoir to maximize hydropower generation without compromising the dam's flood control objective. Optimizing at the daily time step is most suitable when it comes to real-time operations of small and medium-storage dams. A small dam operator is unlikely to make decisions on reservoir releases for such dams at frequencies finer than a day.

2.4.1. Optimization strategy

In general, setting up the reservoir's optimization framework involves three components – 1) advanced scheduling of water releases, 2) useful inflow forecasts that serve as input data, and 3) and optimization model that utilizes forecast information to the best advantage [33]. A major limitation in operating the reservoirs occurs during the flood/peak flow seasons when the high uncertainty in predicting a flood peak leaves the dam operator uncertain on much water to release to balance the various stakeholder benefits. The short-term forecast information was utilized here to provide the operator with a release policy optimized to simultaneously maximize benefits from the conflicting objectives.

To minimize the effect of reduced forecast skill with increasing lead times (see Appendix A), the optimization strategy sequentially updates NWP-based (downscaled by WRF) flow forecasts every other day. Evaluation is performed by calculating optimized hydropower benefits (*optimized* HP) using the optimized releases while passing the observed inflow into the system. The *optimized HP* benefits were compared against the observed benefits (*observed HP*) using observed operations without any optimization/forecasts. The observed benefits correspond to the real-world power generation data obtained from USACE that operates the two dams. The optimized hydropower benefits (megawatt-hours, MWh) were calculated as a product of hydraulic head and power release (via penstocks), considering the turbine efficiency, operating hours and the capacity factor (ratio of actual hydropower produced to the maximum possible over a period).

2.4.2. Optimization objectives and constraints

Reservoir operations were formulated as a Multi-objective Optimization Problem (MOP) based on a Pareto optimal set of solutions with the objective functions of hydropower maximization and flood control [64]. The two objectives are mutually conflicting, since maximizing hydropower production requires higher reservoir storage to produce more power, while for minimization of the flood risk, more water needs to be released to ensure enough storage when the peak inflow hits the reservoir. The Non-dominated Sorting Genetic Algorithm (NSGA-II) [65] was used to yield the Pareto front of the optimal solutions from which an appropriate alternative can be chosen at various satisfaction levels of both the objectives [66]. The two conflicting objectives are formulated below.

1. Minimize the deficit in hydroelectric power production (MW) from the maximum generation capacity of the powerplant (HP_{max}),

$$\min f_1\,(MW) = HP_{max} - \sum_t \varepsilon \cdot \Delta t_{turb} \cdot \left(HF_t - HT_t\right) \cdot R_{p,t} \tag{1}$$

2. Minimize the absolute value of deviations of reservoir elevation (H) from the target rule curve level (T) over the optimization horizon. It is represented as,

$$\min f_2\,(ft) = \sum_t \left|H_t - T_t\right| \tag{2}$$

t – 1–16 days (optimization horizon)
HF – Reservoir forebay water level (ft)
HT – Reservoir tailrace water level (ft)
ε – Turbine efficiency
Δt_{turb} – Turbine operating hours
R_p – Power release from turbines (cfs)

Several constraints were imposed on the optimization problem in the interest of downstream stakeholders, dam safety and environmental concerns. The power and spillway release from the reservoir were limited by the turbine and spillway capacity. The minimum for reservoir storage was set to 95% of the historical minimum and the maximum to the flood control pool while following the storage-volume continuity. The total release was bounded between the environmental flow limit and a safe threshold to prevent flooding at a downstream control station. The mathematical formulation of the constraints is given in Appendix D.

3. Results

Three case studies are presented for forecast-based hydropower maximization using optimized reservoir operations. Two of them were performed over a single storm flow event each for Detroit and Pensacola dams, while a third long-term assessment was performed over a continuous period of ten months for Detroit dam with a long dry spell.

3.1. Detroit Dam – single event assessment

The various pools of the reservoir along with the constraints used in setting up the optimization model are shown schematically in Fig. 6. The maximum total release was set to control the downstream point of Mehama to a threshold of 9000 cfs (255 m^3/s) to prevent downstream flooding.

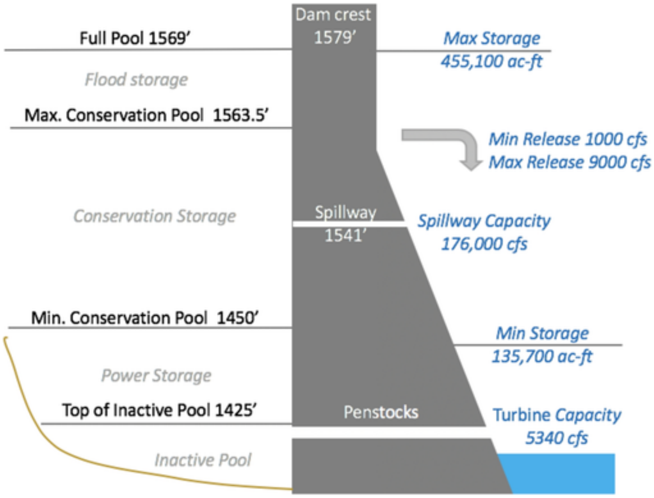

Fig. 6. Cross-section of Detroit dam (not to scale) showing relevant pool elevations (from mean sea level, MSL) along with the optimization constraints obtained from US-ACE. (1 ft = 0.305 m, 1 cfs = 0.028 m^3/s, 1 ac-ft = 1233.48 m^3).

The flow event of 21 Dec 2014 with peak inflow of 24,170 cfs (684 m^3/s) (yearly-scale magnitude) was selected. As the turbine operating characteristics vary over an event or a season, model for hydropower estimation (MWh) based on available daily energy generation data (MW) was developed. Linear regression was performed between the energy generation (in MWh) and the product of hydraulic head ΔH and power release R_p (correlation coefficient, $R^2 = 0.93$) to obtain an average estimate of 19.72 h for turbine's operating hours coupled with its efficiency (the constant $\varepsilon \cdot \Delta t_{turb}$ in Eq. (1)). Although the linear model gives a reasonable approximation for hydropower production function, detailed data on the turbines' characteristic curves and their operating schedules will be sought from dam operating agencies in a future work.

The 16-day forecast inflow obtained using the VIC model forced with WRF-downscaled forecasts for lead times of 3, 5 and 9-days over the selected event are shown in Fig. 7(a).

The optimized release policy was obtained with the optimization starting on Dec 11. A set of 100 non-dominated points on the tradeoff curve (Pareto front) obtained between the two competing objectives are shown in Fig. 7(b) for the first day of optimization. A balanced optimum solution was chosen on the Pareto front giving equal priority for hydropower deficit and flood risk (in terms of deviation from rule curve) and aiming at concurrently minimizing both the objectives. The conflicting nature of the two objectives can be clearly observed from the shape of the Pareto curve.

The optimal release of the first two days were implemented while the later ones were revised in the next model run on Dec 13 using updated forecasts. The sequential updating of forecasts was continued every alternate day until Dec 19. This resulted in the optimized release as shown in Fig. 8 (a). While the releases and elevations from Dec 11–19 are obtained by sequentially updating the forecasts, the

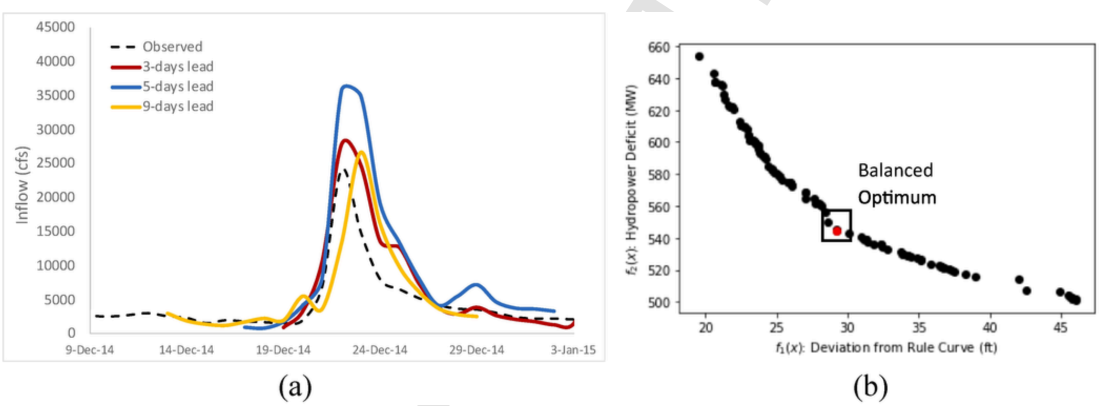

Fig. 7. (a) VIC-modeled 16-day forecast flow forced with WRF-downscaled forecast fields, for lead times of 3, 5 and 9 days for Detroit dam, OR; (b) Non-dominated solutions on the Pareto front and the selected balanced optimum obtained between the objectives of hydropower deficit and deviation from rule curve (to be minimized). (1 cfs = 0.028 m^3/s).

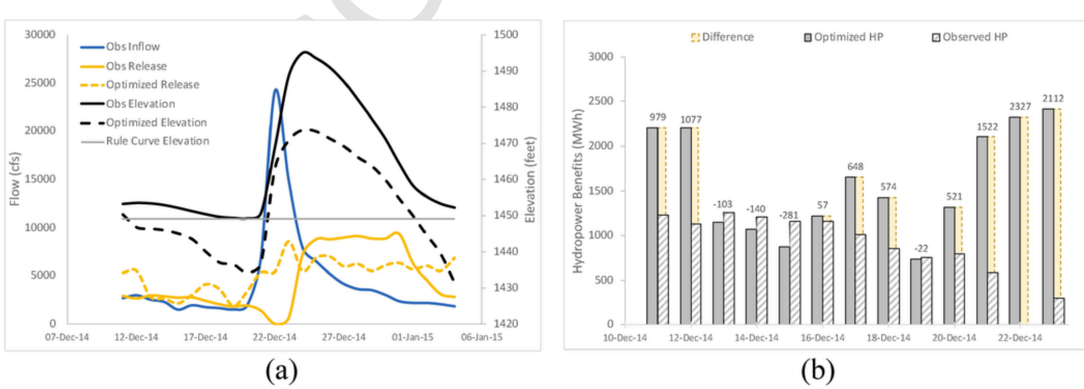

Fig. 8. (a) Optimized releases and elevations from the sequentially updated forecasts from Dec 11–19, along with the respective observed values, (b) Daily comparison of hydropower benefits (MWh) from optimized and observed operations (Detroit dam, OR). 'HP' stands for Hydropower; yellow bars and labels show the difference in benefits from the two set of operations.

values afterwards are obtained from the last optimization run of Dec 19.

As can be seen from Fig. 8(a), the optimized operations result in a higher release as soon as the peak inflow is forecasted due to which the reservoir levels (black dashed curve) drop down within dam's safety limits, and then surges as the peak hits the reservoir. The elevation at the end of the optimization period, however, has a slightly higher deviation from the rule curve (compared to the observed value) as the sequential updates to forecasts have only been made till Dec 19. An *optimized hydropower benefit* of 20,720 MWh was obtained in comparison to the observed production of 11,450 MWh over Dec 11–23. Thus, an additional benefit of 9,270 MWh of hydropower could have been generated before and during the peak inflow event based on weather forecasts and optimization. The daily comparison of hydropower benefits from the optimized and observed operations is shown in Fig. 8(b).

3.2. Pensacola Dam – single event assessment

Similar to Detroit dam, we identified the dam's relevant pools, the operating constraints and turbine features, as depicted in Fig. 9. The optimization constraints for Pensacola dam were obtained from USACE. For the maximum total release, the threshold of 30,000 cfs (849 m^3/s) was selected as a flood-safe value of streamflow at the downstream USGS gage of Neosho River (site ID - 07190500). Other constraints are summarized in Appendix D.

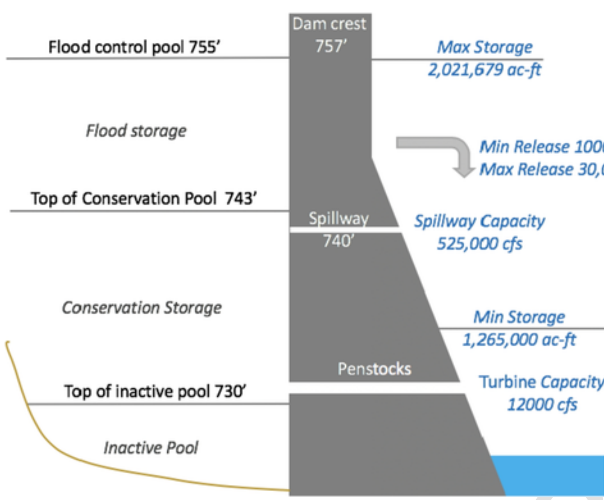

Fig. 9. Cross-section of Pensacola dam (not to scale) showing relevant elevations (from mean sea level, MSL) and the selected constraint values obtained from USACE. (1 ft = 0.305 m, 1 cfs = 0.028 m^3/s, 1 ac-ft = 1233.48 m^3).

The inflow event of 22 Mar 2012 with a peak flow of 82,350 cfs (2332 m^3/s) was chosen for Pensacola dam. As the actual hydropower data (MWh) is not provided on USACE data portal, an estimate of turbine's operating hours and efficiency could not be obtained. Hence, a value, close to that for Detroit, of 20 h was chosen for the constant in hydropower equation $\left(\varepsilon \cdot \Delta t_{turb}\right)$ (Eq. (1)), as both the dams have similar installed hydropower capacities. The 16-day forecast inflow modeled for lead times of 3, 5 and 9-days is shown in Fig. 10(a).

The Pareto front with the non-dominated solutions and the chosen balanced optimum is shown in Fig. 10(b). The optimization based on sequential updates to WRF forecasts for this dam revealed *optimized hydropower benefit* of 31,650 MWh from Mar 11–24, as compared to the *observed benefit* of 18,825 MWh. Again, an additional production of 12,825 MWh pre- and over the peak flow event was realized. The optimized releases and reservoir elevations are compared with the respective observed values in Fig. 11(a) and the daily hydropower benefits plotted in Fig. 11(b).

3.3. Long-term assessment of hydropower benefit

To put our concept to test in the practical world, the reservoir operations model for hydropower maximization using WRF-downscaled forecasts was automated through an online decision support system (see http://depts.washington.edu/saswe/damdss) for Detroit dam. The long-term results obtained from Dec 2017 to Sep 2018 (10 months), consist of both wet and dry seasons. A 16-day optimized operation schedule was derived using the WRF model's downscaled GFS forecasts. Using the actual inflow that occurred during the day and the respective optimized releases, final reservoir storage was computed by satisfying the storage-volume continuity (see Appendix D). The final storage of the first day served as the next day's beginning storage to obtain the next set of optimized releases using the updated forecasts. The model was run for all the ten months using such daily sequential updates. A similar update process was followed by Ref. [75] at a weekly scale. The inflow forecasts generated over the selected 10-month period are compared with the observed values in Appendix B.

The hydropower benefits from the optimized operations were compared with the observed power generation data from USACE in Fig. 12, plotted together with the respective inflow and release. The plots suggest that during the peak flow seasons, optimized policy re-

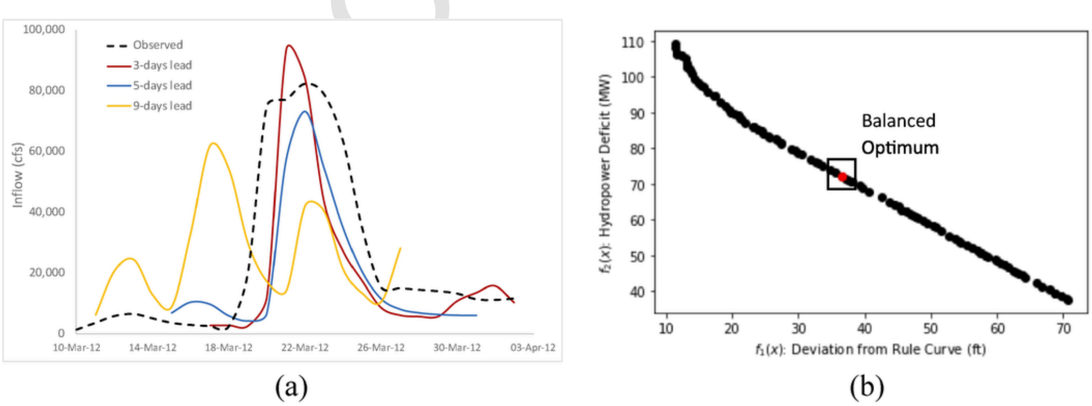

Fig. 10. (a) VIC-modeled 16-day forecast flow, forced with WRF-downscaled forecast fields, for lead times of 3, 5 and 9 days; (b) Pareto front and the selected balanced optimum obtained between the two objectives, Pensacola dam, OK.

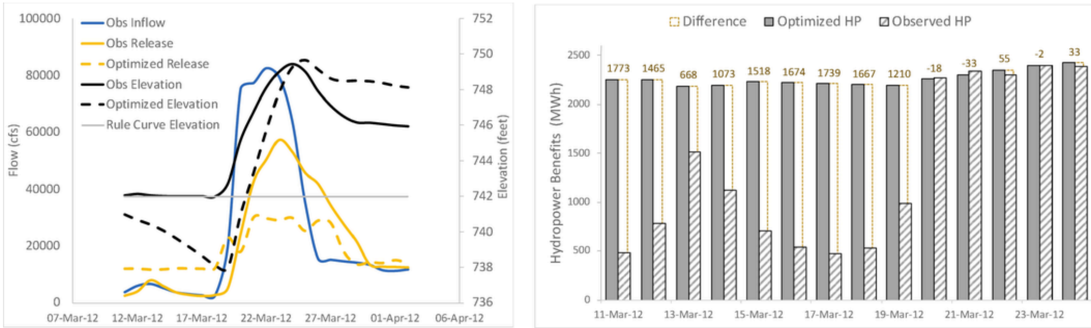

(a) (b)

Fig. 11. (a) Optimized releases and elevations updating forecasts every alternate day from March 11–17, with the respective observed values; (b) Daily comparison of hydropower benefits (MWh) obtained using observed and optimized operations (Pensacola dam, OK). 'HP' stands for Hydropower; yellow bars and labels show the difference in benefits from the two set of operations.

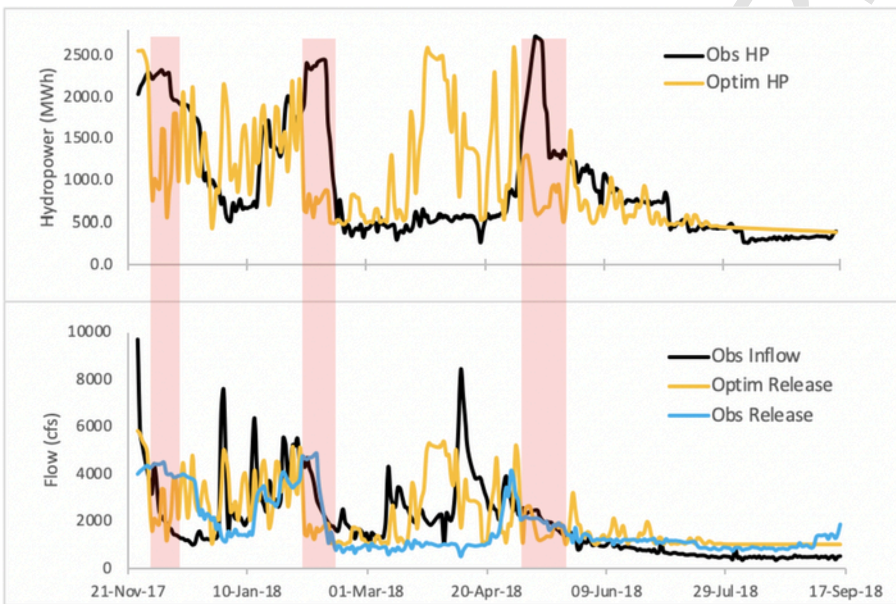

Fig. 12. Optimized hydropower benefits obtained by sequentially updating forecasts every day for Detroit dam, compared with the observed benefits (top); optimized and observed release policy compared along with the observed inflow (bottom). Red bands highlight the days when optimized power was exceeded by the observed power generation.

sults in higher release ahead of the event leading to higher energy generation. For low flows, the optimized release is constrained by the environmental flow limit of 1000 cfs, although the actual operations go below this limit on a few days. The total optimized hydroelectric energy (*optimized HP*) of 258,120 MWh was obtained over the 10-month period in comparison to the observed benefit (*observed HP*) of 244,490 MWh. Thus, an additional hydropower benefit of 13,630 MWh (optimized minus observed hydropower) was obtained over the longer term that included both wet and dry seasons. The highest benefits in energy were obtained during peak inflow occurence, as that is when the dam operator is most uncertain on the release to be made often leading to 'missed hydropower.' There are also episodes when the energy generation from observed operations exceeded the optimized ones (vertically highlighted bands in Fig. 12) that occur during low flow periods, generally after a peak inflow event. This is because, during peak inflow, dam operations hold the water back for preventing the flood downstream due to high uncertainty in future flows. Once the peak flow recedes, the dam operator is bound to release more water brought in by the peak flow event, which increases hydropower production, but also causes high spillway releases increasing downstream risk of flooding. The optimized operations, on the other hand, use the forecasts to pre-release the water already stored before the peak arrives at the reservoir in a controlled manner without causing spill. This generates a consistent amount of energy before and after the peak flood event. The other objectives (of flood control and dam safety) were also not compromised by keeping the reservoir below the safe release threshold of downstream flooding and satisfying the environmental flow constraints. Thus, in a longer period, the concept has potential in producing more energy benefits with reduced flood risk, overcoming the concerns of false alarms and false low flows, when operationalized in real-time operations over the existing infrastructure.

4. Improvements in NWP-based reservoir inflow forecasting technique

As the premise of this research is to elucidate the value of short-term forecasts in hydropower maximization, rather than the value of hydrologic modeling, our prescribed approach needs to be model-agnostic. To demonstrate this, two additional reservoir forecast modeling techniques are described next – one that uses ensemble of NWP-based forcings to generate probabilistic flow forecasts and other that uses a data-based approach to forecasting reservoir inflow.

4.1. NWP-based probabilistic inflow forecasts

To incorporate the uncertainty in forecasts, an ensemble of streamflow forecasts was obtained based on Global Ensemble Forecast System (GEFS) forcings. The 21-member ensemble forecast fields from GEFS were used to force the VIC hydrological model and obtain ensemble of inflow forecasts for 1–16 days. The peak flood event of Mar 2012 over Pensacola dam was chosen for demonstrating the value of available NWP ensemble fields in capturing the uncertainty in flow forecasts. The mean, minimum and maximum forecast flow from the 21-member GEFS ensembles for lead times of 3, 5, 7 and 9 days is shown in the Fig. 13 for the peak flow event. A comparison of forecasting accuracy based on the average GEFS scenario against WRF-downscaled GFS is shown in Table 2, which suggests clear benefits of using probabilistic forecasts likes GEFS over the WRF simulation.

4.2. Data-based approach for inflow forecasts

As the macroscale VIC model leaves room for improvement in modeling accuracy, the data-based technique of Artificial Neural Networks (ANN) was employed for 1–7 days lead reservoir inflow forecasting. ANN, over the last two decades, has been established as an efficient choice for modeling water resource variables while capturing the nonlinearity in flow [83,84]. A three-layered ANN was designed using NWP forecast fields, antecedent streamflow, baseflow and precipitation as the input predictors (refer to Ref. [85] for details). The use of basin-averaged NWP fields alleviates the need of computationally expensive dynamic downscaling using WRF. The ANN model and results of forecasting are briefly presented in Appendix C.

5. Discussion

5.1. Performance assessment - hydropower versus flood control benefits

In order for the proposed optimization strategy to be effective, the two competing objectives of hydropower and flood control need to be

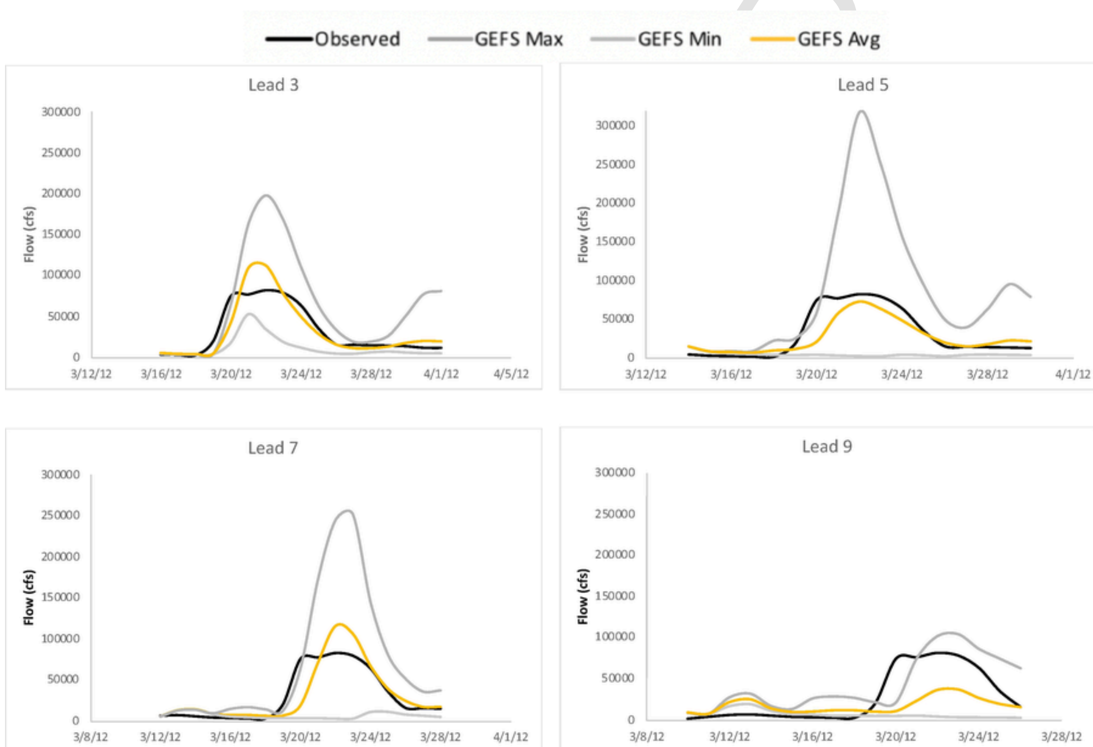

Fig. 13. Ensemble forecast inflow corresponding to mean, minimum and maximum of the 21 ensemble members of GEFS forecast fields over Mar 2012 event for Pensacola dam.

Table 2
Comparison of the forecast flow performance from average GEFS scenario and WRF-downscaled GFS fields over Mar 2012 event for Pensacola dam.

Metric	L3		L5		L9	
	WRF	GEFS	WRF	GEFS	WRF	GEFS
Correlation	0.817	0.905	0.556	0.887	0.002	0.691
RMSE (cfs)	20827.0	14977.1	28407.2	15964.9	34934.1	28298.5
NRMSE	0.678	0.501	0.908	0.515	1.090	0.868

satisfied simultaneously. For the Pensacola dam, during the Mar 2012 peak event, the proposed optimization strategy was able to generate an additional 12,825 MWh of energy on top of the production from observed operations. This amounts to a revenue of $1,251,720 using the average residential electricity rate of 9.76¢/kWh in Oklahoma City [67]. At an average electricity consumption of 900 kWh per month per US household, this additional energy can fulfill the demands of around 11,545 more households for one month. For the competing flood control objective, the performance was assessed from the reduction in the outflow peak over the event. For the selected event, a maximum observed release of 57,211 cfs (1620 m^3/s) was limited to just 30,000 cfs (849 m^3/s) (~47.5% reduction) as a safe threshold to prevent flooding downstream.

For Detroit dam's single event assessment, the proposed optimized operations were able to generate an additional 9,270 MWh of hydropower (on top of the observed value). Again, this energy equivalent to revenue of $908,460 at a rate of 9.8¢/kWh in Oregon [68] that can power up to 8,345 US households for a month. For the long-term assessment over ten months (with inflows lower than the considered individual peak events), the additional energy amounted to 13,630 MWh (5.6% increase over the observed energy) and the optimization strategy was most effective during the high inflow periods. The reservoir release was kept under the flood-safe limit of 9000 cfs (255 m^3/s) for the downstream control station. Thus, the proposed optimization strategy not only generates more hydroelectric power but also addresses the other key objective of reducing the flood risk.

The two dams for the case study assessments were chosen in different hydrological regimes with varying characteristics. As the Detroit dam lies in with steep terrain with small sized basin and fast hydrological response, the rainfall quickly gets converted into runoff with a lesser time of concentration. However, Pensacola dam possesses a flatter terrain with longer rivers resulting in higher time of concentration. Thus, the successful assessment over both the dams, over individual high inflow events as well as operationally over longer term, illustrates the robustness of the concept.

5.2. Scalability of hydropower maximization

While the dams selected for study have different hydrologic regimes, catchment characteristics and reservoir inflows, the variation is certainly much higher across the dams over U.S. and the globe. This variation cannot be captured by the analysis presented in this study. Also, this study was limited in terms of the computational resources to simulate WRF model (for downscaling GFS forcings and generating inflow forecasts) for a year-long period over the Pensacola Dam. This will be considered in a future study by using computationally efficient ANN, as demonstrated here, to forecast inflows and optimize reservoir operations. The practitioners are encouraged to study and extend the framework of optimization to improve the hydropower generation scenario using weather forecast information over other dams suitable for such kind of exploration. These include the dams that are (a) powered, (b) have small to medium reservoir storage capacity, and (c) upstream in the dam network receiving unregulated flow. Our analysis over the U.S. dams revealed 525 dams satisfying these criteria, amounting to 23% of the 2248 powered dams [69]. These dams are shown in Fig. 14 and are the sites for further exploration of their suitability for the concept. We believe that the concept, if extended to a good fraction of such dams, has the potential to bring the nation closer to an energy infrastructure independent of the fossil fuels and other non-renewable sources.

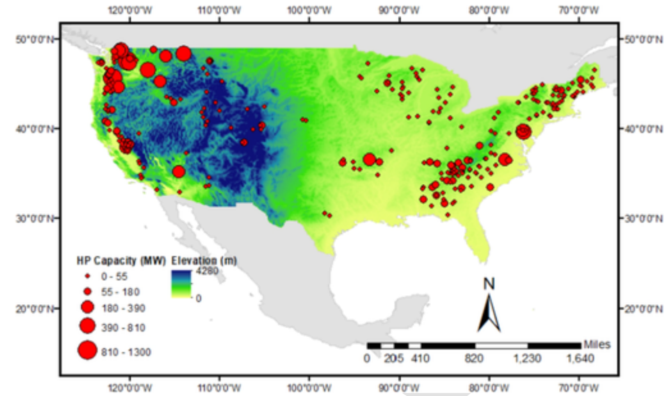

Fig. 14. Locations of upstream dams receiving unregulated inflow to be explored of their suitability for weather forecast use in optimizing reservoir operations.

6. Conclusions

The purpose of this study was to evaluate the potential of short-term weather forecasts to extract more hydroelectric energy, without compromising other competing objectives. The NWP model-based weather forecasts, their dynamic downscaling, hydrologic modeling, and the optimization algorithm were coupled with reservoir operations model to obtain the optimized release policy for maximizing energy production. The concept was demonstrated over Detroit and Pensacola dams with varying hydrological characteristics receiving unregulated inflow. Performance assessment over two-year return period storm events produced benefits of 12,825 and 9,270 MWh for Pensacola and Detroit dams, respectively, while optimization over a longer ten-month period (of wet and dry seasons) for Detroit dam raised the total energy production by 5.6% over the observed scenario. The optimization not only improved hydropower generation, but also helped satisfy the goals of flood control and dam safety. The Pareto optimality allows the operator to choose an appropriate optimal solution depending on the prevailing circumstances in operating the reservoir. It should be noted that, at least for the type of dams demonstrated here, the forecasts help the most during the peak flow (wet) period when uncertainty in the reservoir inflow is high causing over-conservative operations. Nevertheless, the long-term benefits of maximizing the hydropower every day, even in small amounts, is a low-hanging fruit that should not be overlooked, rather be explored to its depth to realize a more sustainable framework for reducing the dependence on fossil-fuel based energy generation. Future research needs to integrate the power demand forecasting with the reservoir operations model so that the opportunity to generate additional power is not missed during times of peak demand.

The value and robustness of NWP forecast fields in deriving the inflow forecasts was further demonstrated using two additional techniques. The 21-member ensemble GEFS forecast fields forced VIC model to generate probabilistic reservoir inflow forecasts over a peak inflow event for Pensacola dam. The average GEFS scenario performed better than the WRF downscaled forecasts. The improved inflow forecasts with the uncertainty estimates (from probabilistic forecasts) can benefit the optimization model and arrive at optimal decisions different confidence levels. Secondly, the data-based approach of ANN was used to forecast short-term inflow over the two dams. ANN improved the skill in inflow forecasting as well as proved to be computationally efficient. Future work will integrate these two approaches with the reservoir operations optimization model.

Combining optimization and simulation models for managing water resources in a real-world setting has not been fully realized yet [74]. By using real data on real dams with real-world constraints, we have demonstrated very clearly that the currently available weather forecasts from NWP models have a lot to offer to address energy security. Thanks to the advances in atmospheric science and modeling, these weather forecasts are already available publicly. The challenge now is to convert availability to accessibility so that dam operators can operate based on an improved advisory that makes hydropower generation more efficient (more power with same or less impounded water) and reduce our impact on the natural world.

Acknowledgement

The authors acknowledge the guidance and contribution of Dr. Chris Frans of US Army Corps of Engineers (USACE) Seattle District. The authors are grateful for support received from Ivanhoe Foundation and NASA Surface Water Ocean Topography (SWOT) mission.

Appendix A. WRF performance evaluation

The evaluation of dynamically downscaled forcings of precipitation, min/max temperature and wind speed from WRF was performed using Livneh daily CONUS near-surface gridded meteorological dataset [70]. For Detroit dam, due to the absence of Livneh dataset after 2014, WRF model evaluation was performed for the peak flow event of 16 January 2011. In the case of Pensacola dam, WRF model was set up for the peak inflow event of 20 March 2012. The GFS forecast fields corresponding to lead times of 1–16 days was processed for downscaling using WRF simulation for both the dams. The metrics of correlation, RMSE, Probability of detection (POD) and Frequency Bias [55] were calculated to assess the performance of downscaled variables at different lead times. POD is the measure of how well the simulation can capture the true positives while frequency bias measures the extent to which the simulated results are biased towards false positive/negative (both having best value of 1). For both dams, performance of the forecast model deteriorates with lead time, with higher number of misses (true negatives) and false positives. The comparison maps of precipitation are shown in Fig. A1 for the selected peak flow events and Table A1 summarizes metrics for both the dams. Results for lead times of 3, 5 and 7 days for Detroit dam, and of 4, 6 and 8 days for Pensacola dam are shown here.

Table A1 Metrics for evaluation of WRF downscaled forcings for lead times of 3–8 days (L3-L8).

Variable	Metric	Detroit Dam			Pensacola Dam		
		L3	L5	L7	L4	L6	L8
Precipitation	Correlation	0.85	0.84	0.19	0.61	0.31	−0.09
	RMSE (mm)	11.18	21.62	15.86	23.39	30.52	33.57
	POD	0.93	0.96	0.04	0.72	0.66	0.57
	Freq. Bias	2.28	2.56	0.04	0.76	0.67	0.58
Max. Temperature	Correlation	0.53	0.48	0.48	0.78	0.71	0.64
	RMSE (˚C)	4.88	4.65	6.05	3.73	4.82	5.19
Min. Temperature	Correlation	0.68	0.67	0.68	0.87	0.82	0.58
	RMSE (˚C)	5.45	5.34	3.46	2.07	2.26	3.23
Wind Speed	Correlation	0.16	0.36	0.01	0.61	0.45	−0.19
	RMSE (m/s)	2.26	2.03	2.56	1.70	1.88	2.76

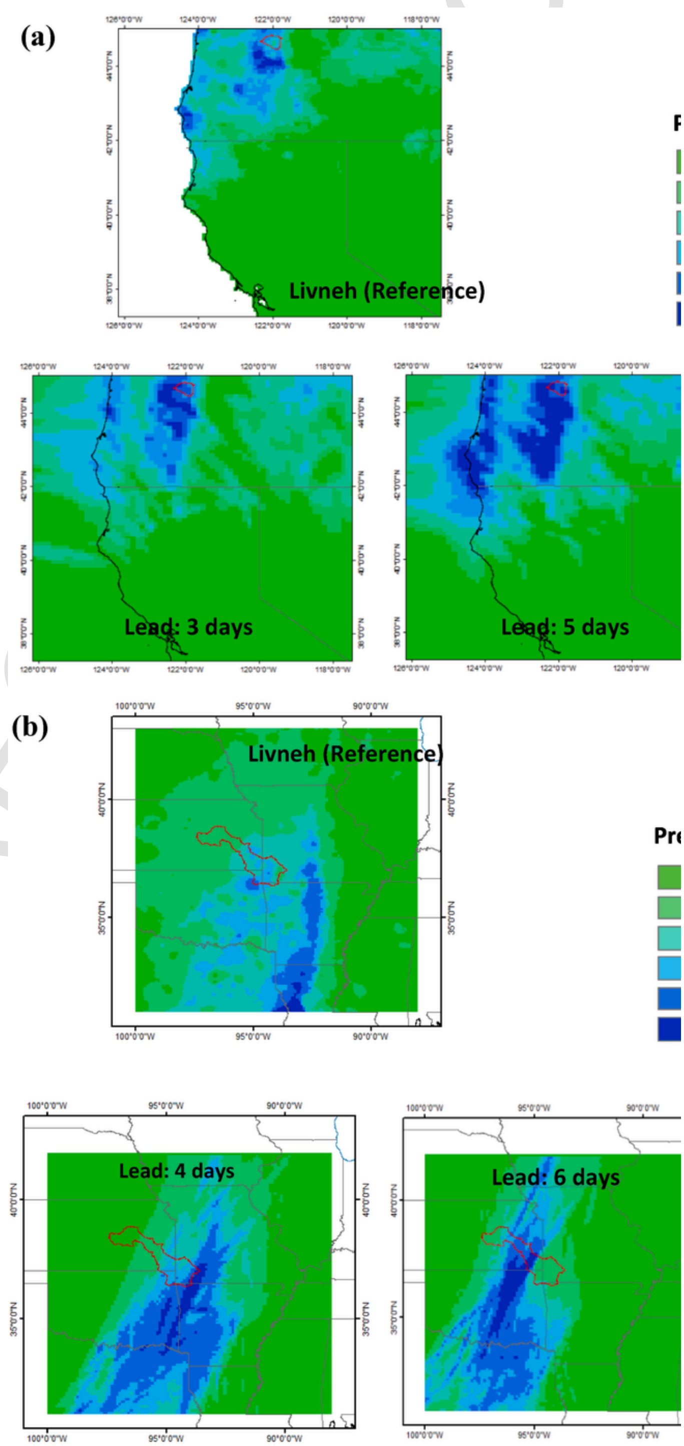

Fig. A1. Assessment of WRF downscaled precipitation (0.1°) with reference Livneh dataset over the events of 16 Jan 2011 and 20 Mar 2012 for (a) Detroit and (b) Pensacola dam.

Appendix B. VIC Model Setup

Detroit Dam

Calibration was performed on the period from 2009 to 11, and the validation over 2013–15. The first few months were ignored for calculating metrics considering the model spin-up period. Normalized RMSE is calculated as $\frac{RMSE}{\sigma_{obs}}$ (where σ_{obs} is standard deviation of the observed streamflow). The results for calibration and validation are shown in Fig. B1. As the high flow events are of interest, normalized mean absolute error $\left(NMAE = \frac{1}{Num\ of\ peaks} \sum \frac{|Obs-Mod|}{Mod}\right)$ specific to peaks (with flow exceeding turbine capacity of 9000 cfs) and percentage of times peaks were under/overestimated are also shown in Fig. B1.

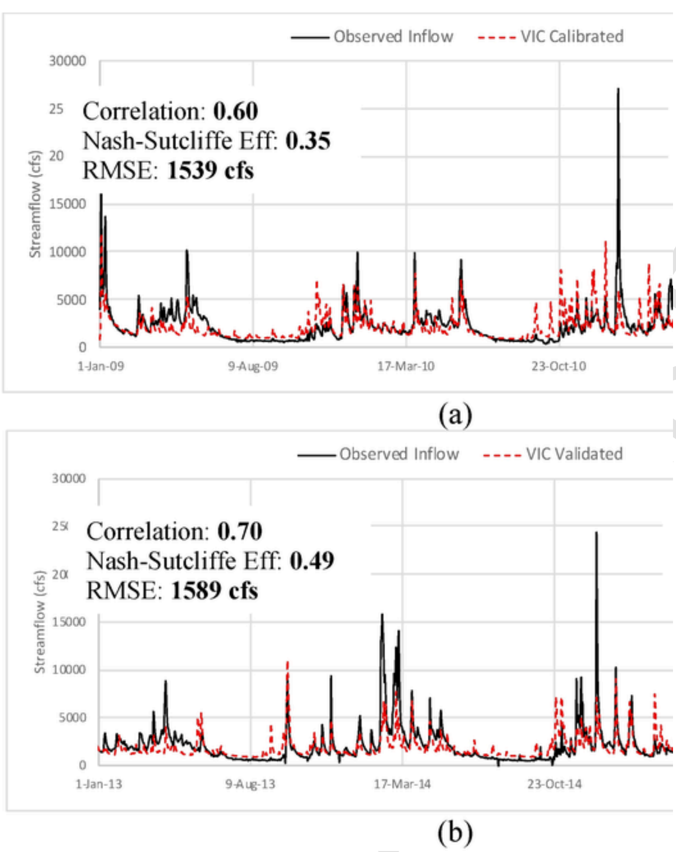

Fig. B1. (a) VIC calibrated and (b) validated streamflow, along with metrics for Detroit Dam. NMAE is normalized mean absolute error, UE/OE is % times peak is under/overestimated. (1 cfs = 0.028 m^3/s)

Pensacola Dam

Daily inflow data from 2002 to 06 was used for calibration, while validation was performed over 2011–15. The calibration and validation results are shown below in Fig. B2. The NMAE and percent times peak is overestimated (false positive) or underestimated (missed bias) over the considered period is obtained for events with flow exceeding 20,000 cfs (566 m^3/s).

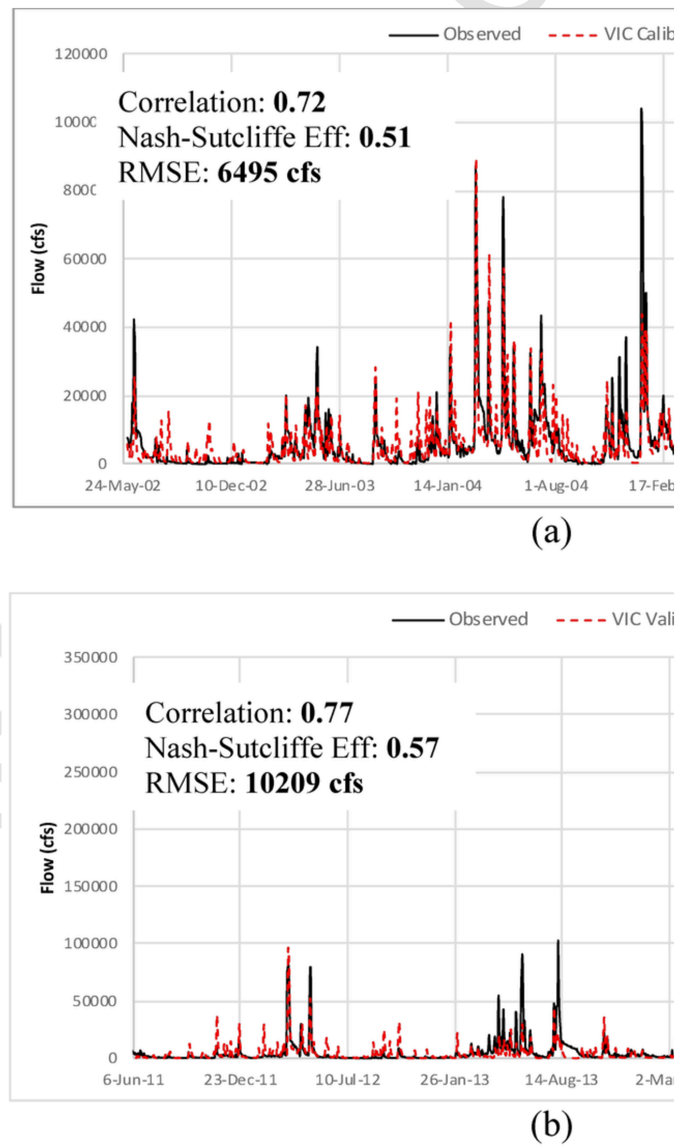

Fig. B2. (a) VIC calibrated and (b) validated streamflow, with metrics for Pensacola Dam. NMAE is normalized mean absolute error, UE/OE is % times peak is under/overestimated. (1 cfs = 0.028 m^3/s).

The performance of VIC model for Pensacola dam was better compared to that of Detroit dam. Running this macroscale model at 0.1° resolution for smaller basin of Detroit dam results in very few grid cells that cannot capture the sub-grid heterogeneity for modeling the hydrologic variables.

The modeled real-time reservoir inflow forecasts over the Detroit dam generated by the operational system over Dec 2017 to Sep 2018, forcing the VIC model with WRF downscaled forcings, is compared with the observed inflow in Fig. B3. The hindcast flow from VIC model is also plotted alongside for comparison. The metrics of comparison are summarized in Table B1.

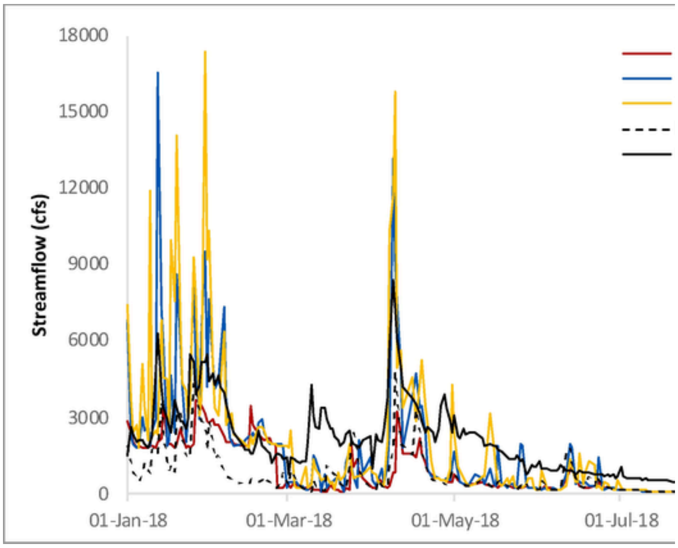

Fig. B3. Comparison of the modeled daily forecast/hindcast flow for lead times of 1, 4 and 7 days over Jan–Sep 2018 against observed data for Detroit dam. (1 cfs = 0.028 m^3/s)

Table B1 Metrics for comparison of daily modeled forecast/hindcast flows against observed data over Jan–Sep 2018 for Detroit dam.

	Best value	Lead 1	Lead 4	Lead 7	Lead 10	Hind-cast
RMSE (cfs)	0.0	1486.1	1459.8	1944.7	1882.3	1504.0
NRMSE	0.0	1.03	1.01	1.35	1.31	1.04
Correlation	1.0	0.64	0.78	0.71	0.67	0.72
NSE	1.0	0.35	0.37	−0.11	−0.04	0.34

Appendix C. Data-based Inflow Forecasting based on NWP Forecasts

The selected ANN architecture consisted of antecedent precipitation (2 days), antecedent baseflow (3 days), antecedent streamflow (3 days; for lead times of 4–7 days), antecedent moving average streamflow (3-, 5- and 8-day window based on lead time), forecast precipitation (1 day) and forecast min/max temperature (1 day each). For details on the setup of ANN model, please refer to Ref. [85]. Fig. C1 plots the ANN forecasted flow against observed values over the validation period (2016–17) for 1, 4, and 7-days lead time Detroit and Pensacola dams. The metrics of NSE, Correlation and Normalized RMSE are tabulated in Table C1.

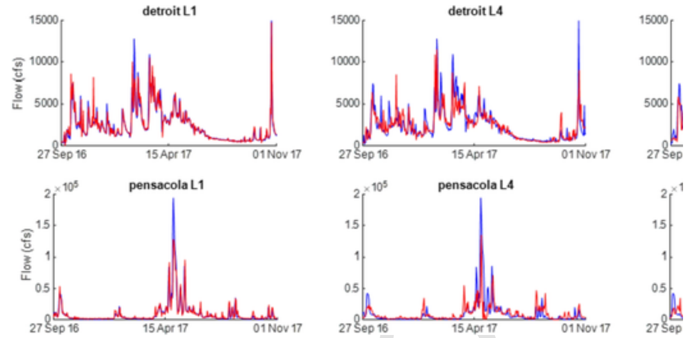

Fig. C1. ANN modeled flow plotted against observed values for 1, 4, and 7-days lead time (L1, L4, and L7) for Detroit and Pensacola dams.

Table C1 Evaluation metrics for the ANN forecasted flow for three lead times

Dam Name	NSE			Correlation			NRMSE	
	L1	L4	L7	L1	L4	L7	L1	L4
Detroit	0.843	0.720	0.606	0.920	0.849	0.780	0.264	0.3
Pensacola	0.838	0.517	0.268	0.922	0.724	0.519	0.312	0.5

Appendix D. Constraints for Optimization

1. Release from the turbines is constrained by the turbine capacity, P_{turb}.

$$R_{p,t} \leq P_{turb} \ , \ \forall t \tag{D1}$$

2. The system follows storage-volume continuity (water-balance equation) which requires that in each period t,

$$S_{t+1} = S_t + \left[I_t - L_t - \left(R_{p,t} + R_{np,t} \right) \right] \cdot \Delta t, \ \ \forall t \tag{D2}$$

However, as the optimization is performed at daily time steps ($\Delta t = 1$), the losses due to evaporation and seepage, L_t, were ignored.

3. Reservoir storage (S) was limited to ensure dam safety and avoid infeasible scenarios such as the reservoir running empty,

$$S_{min} \leq S_t \leq S_{max}, \ \ \forall t = 1, 2, \ldots, 16 \tag{D3}$$

4. Daily hydropower production (HP) was limited by the powerplant's overload capacity (HP_{max}),

$$HP_t < HP_{max}, \ \ \forall t = 1, 2, \ldots, 16 \tag{D4}$$

5. To prevent the downstream flooding hazards, the total release was constrained to a maximum limit, R_{max},

$$R_{p,\,t} + R_{np,t} \le R_{max},\ \forall t \tag{D5}$$

6. To avoid excessive and infeasible rates of non-power release via the spillway, the non-power release rate was limited to the spillway capacity,

$$R_{np,t} \le Spill_{max},\quad \forall t \tag{D6}$$

7. Lastly, the releases made from reservoir should comply with the environmental flow limit, Q_{env},

$$R_{np,\,t} + R_{p,t} \ge Q_{env},\ \forall t \tag{D7}$$

Table D1 Parameters/constraints for the optimization model setup for the two dams.

Parameters	Detroit Dam	Pensacola Dam
Turbine Capacity	$151.2\,m^3/s$ (5340 cfs)	$340\,m^3/s$ (12,000 cfs)
Spillway Capacity	$4{,}984\,m^3/s$ (176,000 cfs)	$14{,}866\,m^3/s$ (525,000 cfs)
Minimum storage	$1.67\times10^8\,m^3$ (135.7 kaf)	$1.56\times10^8\,m^3$ (126.5 kaf)
Maximum storage	$5.61\times10^8\,m^3$ (455.1 kaf)	$2.4937\times10^9\,m^3$ (2021.7 kaf)
Maximum release	$255\,m^3/s$ (9000 cfs)	$850\,m^3/s$ (30,000 cfs)
Env. flow limit	$42.5\,m^3/s$ (1500 cfs)	$28.3\,m^3/s$ (1000 cfs)

References

[1] M.Z. Jacobson, M.A. Delucchi, Z.A.F. Bauer, S.C. Goodman, W.E. Chapman, et al., 100% clean and renewable wind, water, and sunlight all-sector energy roadmaps for 139 countries of the world, Joule 1 (2017) 108–121, https://doi.org/10.1016/j.joule.2017.07.005.

[2] Hydropower Vision, A New Chapter for America's 1st Renewable Electricity Source, Department of Energy, 2016 https://www.energy.gov/eere/water/articles/hydropower-vision-new-chapter-america-s-1st-renewable-electricity-source, Accessed 21 November 2016.

[3] F. Vieira, H.M. Ramos, Optimization of operational planning for wind/hydro hybrid water supply systems, Renew. Energy 34 (2009) 928–936, https://doi.org/10.1016/j.renene.2008.05.031.

[4] M.Z. Jacobson, Review of solutions to global warming, air pollution, and energy security, Energy Environ. Sci. 2 (2009) 148–173, https://doi.org/10.1039/b809990c.

[5] M.Z. Jacobson, M.A. Delucchi, A.R. Ingraffea, R.W. Howarth, G. Bazouin, et al., A roadmap for repowering California for all purposes with wind, water, and sunlight, Energy 73 (2014) 875–889, https://doi.org/10.1016/j.energy.2014.06.099.

[6] M.Z. Jacobson, M.A. Delucchi, M.A. Cameron, B.V. Mathiesen, Matching demand with supply at low cost in 139 countries among 20 world regions with 100% intermittent wind, water, and sunlight (WWS) for all purposes, Renew. Energy 123 (2018) 236–248, https://doi.org/10.1016/j.renene.2018.02.009.

[7] M.Z. Jacobson, M.A. Delucchi, Providing all global energy with wind, water, and solar power, Part I: technologies, energy resources, quantities and areas of infrastructure, and materials, Energy Policy 39 (2011) 1154–1169, https://doi.org/10.1016/j.enpol.2010.11.040.

[8] D. Heide, L. von Bremen, M. Greiner, C. Hoffmann, M. Speckmann, S. Bofinger, Seasonal optimal mix of wind and solar power in a future, highly renewable Europe, Renew. Energy 35 (2010) 2483–2489, https://doi.org/10.1016/j.renene.2010.03.012.

[9] M.A. Delucchi, M.Z. Jacobson, Providing all global energy with wind, water, and solar power, Part II: reliability, system and transmission costs, and policies, Energy Policy 39 (2011) 1170–1190, https://doi.org/10.1016/j.enpol.2010.11.045.

[10] S. Becker, B.A. Frew, G.B. Andresen, T. Zeyer, S. Schramm, M. Greiner, M.Z. Jacobson, Features of a fully renewable US electricity system: optimized mixes of wind and solar PV and transmission grid extensions, Energy 72 (2014) 443–458, https://doi.org/10.1016/j.energy.2014.05.067.

[11] M.Z. Jacobson, M.A. Delucchi, Providing All Global Energy with Wind, Water, and Solar Power, Part I: Technologies, Energy Resources, Quantities and Areas of Infrastructure, and Materials, 2011https://doi.org/10.1016/j.enpol.2010.11.040.

[12] U.S. Energy Information Administration, Electric Power Monthly: with Data for June 2018, 2018https://doi.org/10.2172/123200, Washington DC.

[13] A.F. Hamlet, D. Huppert, D.P. Lettenmaier, Economic value of long-lead streamflow forecasts for Columbia River hydropower, J. Water Resour. Plan. Manag. 128 (2002) 91–101, https://doi.org/10.1061/(ASCE)0733-9496(2002)128:2(91).

[14] J. Spector, The Environmentalist Case against 100% Renewable Energy Plans - CityLab, 2015 https://www.citylab.com/environment/2015/07/the-environmentalist-case-against-100-renewable-energy-plans/398906/, Accessed 19 March 2017.

[15] B. Sørensen, A combined wind and hydro power system, Energy Policy 9 (1981) 51–55.

[16] D. Egré, J.C. Milewski, The diversity of hydropower projects, Energy Policy 30 (2002) 1225–1230.

[17] I. Kougias, S. Szabó, F. Monforti-Ferrario, T. Huld, K. Bódis, A methodology for optimization of the complementarity between small-hydropower plants and solar PV systems, Renew. Energy 87 (2016) 1023–1030, https://doi.org/10.1016/j.renene.2015.09.073.

[18] T. Grumet, How Germany's Combined Wind and Hydropower Plant Will Work - GE, 2016 https://www.ge.com/reports/unique-combo-wind-hydro-power-revolutionize-renewable-energy/, Accessed 3 December 2017.

[19] Hydropower Vision, A New Chapter for America's 1st Renewable Electricity Source, Department of Energy, 2016 https://www.energy.gov/eere/water/articles/hydropower-vision-new-chapter-america-s-1st-renewable-electricity-source, Accessed 12 October 2017.

[20] Y. Miao, X. Chen, F. Hossain, Maximizing hydropower generation with observations and numerical modeling of the atmosphere, J. Hydrol. Eng. 21 (2016) 2516002, https://doi.org/10.1061/(ASCE)HE.1943-5584.0001405.

[21] J.W. Labadie, Optimal operation of multireservoir systems: state-of-the-art review, J. Water Resour. Plan. Manag. 130 (2004) 93–111, https://doi.org/10.1061/(ASCE)0733-9496(2004)130:2(93).

[22] P. Block, Tailoring seasonal climate forecasts for hydropower operations, Hydrol. Earth Syst. Sci. 15 (2011) 1355–1368, https://doi.org/10.5194/hess-15-1355-2011.

[23] S.-Y. Lee, A.F. Hamlet, C.J. Fitzgerald, S.J. Burges, Optimized flood control in the Columbia River basin for a global warming scenario, J. Water Resour. Plan. Manag. 135 (2009) 440–450, https://doi.org/10.1061/(ASCE)0733-9496(2009)135:6(440).

[24] A. Ficchì, L. Raso, D. Dorchies, F. Pianosi, P. Malaterre, P. Van Overloop, Optimal operation of the multireservoir system in the seine River basin using deterministic and ensemble forecasts, J. Water Resour. Plan. Manag. 142 (2016) 5015005, https://doi.org/10.1061/(ASCE)WR.1943-5452.0000571.

[25] P. Bauer, A. Thorpe, G. Brunet, The quiet revolution of numerical weather prediction, Nature 525 (2015) 47–55, https://doi.org/10.1038/nature14956.

[26] L. Goddard, Y. Aitchellouche, W. Baethgen, M. Dettinger, R. Graham, P. Hayman, M. Kadi, R. Martínez, H. Meinke, Providing seasonal-to-interannual climate information for risk management and decision-making, Procedia Environ. Sci. 1 (2010) 81–101, https://doi.org/10.1016/j.proenv.2010.09.007.

[27] D. Anghileri, N. Voisin, A. Castelletti, F. Pianosi, B. Nijssen, D.P. Lettenmaier, Value of long-term streamflow forecasts to reservoir operations for water supply in snow-dominated river catchments, Water Resour. Res. 52 (2016) 4209–4225, https://doi.org/10.1002/2015WR017864.

[28] K.P. Georgakakos, N.E. Graham, A.P. Georgakakos, H. Yao, Demonstrating Integrated Forecast and Reservoir Management (INFORM) for Northern California in an Operational Environment, IAHS-AISH Publ., 2007439–444.

[29] FIRO_Overview, Center for Western Weather and Water Extremes, 2016 http://cw3e-web.ucsd.edu/firo/, Accessed 31 July 2017.

[30] J. Murphy, Predictions of climate change over Europe using statistical and dynamical downscaling techniques, Int. J. Climatol. 20 (2000) 489–501, https://doi.org/10.1002/(SICI)1097-0088(200004)20:5<489::AID-JOC484>3.0.CO;2-6.

[31] S. Sikder, F. Hossain, Assessment of the weather research and forecasting model generalized parameterization schemes for advancement of precipitation forecasting in monsoon-driven river basins, J. Adv. Model. Earth Syst. 8 (2016) 1210–1228, https://doi.org/10.1002/2016MS000678.

[32] C. Teutschbein, F. Wetterhall, J. Seibert, Evaluation of different downscaling techniques for hydrological climate-change impact studies at the catchment scale, Clim. Dyn. 37 (2011) 2087–2105, https://doi.org/10.1007/s00382-010-0979-8.

[33] W.W.-G. Yeh, Reservoir management and operations models: a state-of-the-art review, Water Resour. Res. 21 (1985) 1797–1818, https://doi.org/10.1029/WR021i012p01797.

[34] D. Rani, M.M. Moreira, Simulation–optimization modeling: a survey and potential application in reservoir systems operation, Water Resour. Manag. 24 (2010) 1107–1138, https://doi.org/10.1007/s11269-009-9488-0.

[35] A. Ahmad, A. El-Shafie, S.F.M. Razali, Z.S. Mohamad, Reservoir optimization in water resources: a review, Water Resour. Manag. 28 (2014) 3391–3405, https://doi.org/10.1007/s11269-014-0700-5.

[36] M. Yasar, Optimization of reservoir operation using cuckoo search algorithm: example of adiguzel dam, Denizli, Turkey, Math. Probl. Eng. 2016 (2016) 1–7, https://doi.org/10.1155/2016/1316038.

[37] M.T.L. Barros, F.T.-C. Tsai, S. Yang, J.E.G. Lopes, W.W.-G. Yeh, Optimization of large-scale hydropower system operations, J. Water Resour. Plan. Manag. 129 (2003) 11, https://doi.org/10.1061/(ASCE)0733-9496(2003)129:3(178).

[38] V. Jothiprakash, R. Arunkumar, Multi-reservoir optimization for hydropower production using NLP technique, KSCE J. Civ. Eng. 18 (2014) 344–354, https://doi.org/10.1007/s12205-014-0352-2.

[39] N.S. Hsu, C.C. Wei, A multipurpose reservoir real-time operation model for flood control during typhoon invasion, J. Hydrol. 336 (2007) 282–293, https://doi.org/10.1016/j.jhydrol.2007.01.001.

[40] J.S. Windsor, Optimization model for the operation of flood control systems, Water Resour. Res. 9 (1973) 1219–1226, https://doi.org/10.1029/WR009i005p01219.

[41] Y. Ji, X. Lei, S. Cai, X. Wang, Hedging rules for water supply reservoir based on the model of simulation and optimization, Water 8 (2016) https://doi.org/10.3390/W8060249, Switzerland.

[42] T.R. Neelakantan, N.V. Pundarikanthan, Hedging rule optimisation for water supply reservoirs system, Water Resour. Manag. 13 (1999) 409–426, https://doi.org/10.1023/A:1008157316584.

[43] P.E. Georgiou, D.M. Papamichail, Optimization model of an irrigation reservoir for water allocation and crop planning under various weather conditions, Irrig. Sci. 26 (2008) 487–504, https://doi.org/10.1007/s00271-008-0110-7.

[44] S.K. Sadati, S. Speelman, M. Sabouhi, M. Gitizadeh, B. Ghahraman, GA-Optimal irrigation water allocation using a genetic algorithm under various weather conditions, Water (Switzerland) 6 (2014) 3068–3084, https://doi.org/10.3390/w6103068.

[45] W.W.-G. Yeh, L. Becker, Multiobjective analysis of multireservoir operations, Water Resour. Res. 18 (1982) 1326–1336, https://doi.org/10.1029/WR018i005p01326.

[46] W. Ding, C. Zhang, Y. Peng, R. Zeng, H. Zhou, X. Cai, An analytical framework for flood water conservation considering forecast uncertainty and acceptable risk, Water Resour. Res. 51 (2015) 4702–4726, https://doi.org/10.1002/2015WR017127.

[47] M.J. Reddy, D.N. Kumar, Optimal reservoir operation using multi-objective evolutionary algorithm, Water Resour. Manag. 20 (2006) 861–878, https://doi.org/10.1007/s11269-005-9011-1.

[48] M.J. Reddy, D. Nagesh Kumar, Multi-objective particle swarm optimization for generating optimal trade-offs in reservoir operation, Hydrol. Process. 21 (2007) 2897–2909, https://doi.org/10.1002/hyp.6507.

[49] S.T. Khu, H. Madsen, Multiobjective calibration with Pareto preference ordering: an application to rainfall-runoff model calibration, Water Resour. Res. 41 (2005) https://doi.org/10.1029/2004WR003041.

[50] L. Le Ngo, H. Madsen, D. Rosbjerg, Simulation and optimisation modelling approach for operation of the Hoa Binh reservoir, Vietnam, J. Hydrol. 336 (2007) 269–281, https://doi.org/10.1016/j.jhydrol.2007.01.003.

[51] M. Ahmadi, O. Bozorg Haddad, M.A. Mariño, Extraction of flexible multi-objective real-time reservoir operation rules, Water Resour. Manag. 28 (2014) 131–147, https://doi.org/10.1007/s11269-013-0476-z.

[52] T.E. Croley, K.N. Raja Rao, Multiobjective risks in reservoir operation, Water Resour. Res. 15 (1979) 807–814, https://doi.org/10.1029/WR015i004p00807.

[53] Query Timeseries from USACE Northwestern Division, Dataquery 2.0, 2017 http://www.nwd-wc.usace.army.mil/dd/common/dataquery/www/, Accessed 17 October 2017.

[54] Monthly Charts for Grand Lake O' the Cherokees, Pensacola Dm, 2018 http://www.swt-wc.usace.army.mil/PENScharts.html, Accessed 21 August 2017.

[55] X. Chen, F. Hossain, Revisiting Extreme Storms of the Past 100 Years for Future Safety of Large Water Management Infrastructures, vol 4, Earth's Futur, 2016306–322, https://doi.org/10.1002/2016EF000368.

[56] W.C. Skamarock, J.B. Klemp, J. Dudhia, D.O. Gill, D.M. Barker, M.G. Duda, X.-Y. Huang, W. Wang, J.G. Powers, A Description of the Advanced Research WRF Version 3, 2008https://doi.org/10.5065/D68S4MVH.

[57] D.J. Stensrud, Parameterization Schemes: Keys to Understanding Numerical Weather Prediction Models, Cambridge University Press, 2007.

[58] Pacific Northwest Mesoscale Model Numerical Forecast Information, 2017 https://www.atmos.washington.edu/wrfrt/info.html, Accessed 23 November 2017.

[59] X. Liang, D.P. Lettenmaier, E.F. Wood, S.J. Burges, A simple hydrologically based model of land surface water and energy fluxes for general circulation models, J. Geophys. Res. 99 (1994) 14415, https://doi.org/10.1029/94JD00483.

[60] X. Liang, E.F. Wood, D.P. Lettenmaier, Surface soil moisture parameterization of the VIC-2L model: evaluation and modification, Glob. Planet. Chang. 13 (1996) 195–206, https://doi.org/10.1016/0921-8181(95)00046-1.

[61] Global Surface Summary of the Day - GSOD, NOAA data catalog, in: https://data.noaa.gov/dataset/global-surface-summary-of-the-day-gsod, 2017Accessed 30 August 2017.

[62] D. Lohmann, R. Nolte-Holube, E. Raschke, A large-scale horizontal routing model to be coupled to land surface parametrization schemes, Tellus Ser. A Dyn. Meteorol. Oceanogr. 48 (1996) 708–721, https://doi.org/10.3402/tellusa.v48i5.12200.

[63] D. Lohmann, E. Raschke, B. Nijssen, D.P. Lettenmaier, Regional scale hydrology: I. Formulation of the VIC-2L model coupled to a routing model, Hydrol. Sci. J. 43 (1998) 131–141, https://doi.org/10.1080/02626669809492107.

[64] H. Madsen, B. Richaud, C.B. Pedersen, C. Borden, A real-time inflow forecasting and reservoir optimization system for optimizing hydropower production, Waterpower XVI (2009) 1–12.

[65] K. Deb, S. Agrawal, A. Pratap, T. Meyarivan, A fast elitist non-dominated sorting genetic algorithm for multi-objective optimization: NSGA-II, In: International Conference on Parallel Problem Solving from Nature, Springer, Berlin, Heidelberg, 2000, pp. 849–858.

[66] F.F. Li, J. Qiu, Multi-objective reservoir optimization balancing energy generation and firm power, Energies 8 (2015) 6962–6976, https://doi.org/10.3390/en8076962.

[67] Oklahoma City, OK Electricity Rates | Electricity Local, 2018 https://www.electricitylocal.com/states/oklahoma/oklahoma-city/, Accessed 21 August 2018.

[68] Oregon Electricity Rates | Electricity Local, 2018 https://www.electricitylocal.com/states/oregon/, Accessed 11 May 2018.

[69] NHAAP | Existing Hydropower Assets, 2017 https://nhaap.ornl.gov/existing_hydropower_assets, Accessed 8 December 2017.

[70] B. Livneh, E.A. Rosenberg, C. Lin, B. Nijssen, V. Mishra, K.M. Andreadis, E.P. Maurer, D.P. Lettenmaier, A long-term hydrologically based dataset of land surface fluxes and states for the conterminous United States: update and extensions, J. Clim. 26 (2013) 9384–9392, https://doi.org/10.1175/jcli-d-12-00508.1.

[71] W.H. Farmer, R.M. Vogel, On the deterministic and stochastic use of hydrologic models, Water Resour. Res. 52 (2016) 5619–5633, https://doi.org/10.1002/2016WR019129.

[72] F. Hossain, A.M. Degu, W. Yigzaw, S. Burian, D. Niyogi, J.M. Shepherd, R. Pielke, Climate feedback–based provisions for dam design, operations, and water management in the 21st century, J. Hydrol. Eng. 17 (2012) 837–850, https://doi.org/10.1061/(ASCE)HE.1943-5584.0000541.

[73] B. Lehner, C.R. Liermann, C. Revenga, C. Voro Smarty, B. Fekete, P. Crouzet, et al., Global Reservoir and Dam (GRanD) Database, Version 1.1, Global Water System Project, Bonn, Germany, 2011.

[74] G.M. Sechi, A. Sulis, Water system management through a mixed optimization-simulation approach, J. Water Resour. Plan. Manag. 135 (2009) 160–170, https://doi.org/10.1061/(ASCE)0733-9496(2009)135:3(160).

[75] E.T. Alemu, R.N. Palmer, A. Polebitski, B. Meaker, Decision support system for optimizing reservoir operations using ensemble streamflow predictions, J. Water Resour. Plan. Manag. 137 (2011) 72–82, https://doi.org/10.1061/(ASCE)WR.1943-5452.0000088.

[76] Global Forecast System (GFS), National Centers for Environmental Information (NCEI) Formerly Known as National Climatic Data Center, NCDC, 2018 https://www.ncdc.noaa.gov/data-access/model-data/model-datasets/global-forcast-system-gfs, Accessed 30 December 2017.

[77] M. Liu, L. Tan, S. Cao, Theoretical model of energy performance prediction and BEP determination for centrifugal pump as turbine, Energy 172 (2019) 712–732.

[78] Y. Liu, L. Tan, Tip clearance on pressure fluctuation intensity and vortex characteristic of a mixed flow pump as turbine at pump mode, Renew. Energy 129 (2018) 606–615.

[79] Y. Hao, L. Tan, Symmetrical and unsymmetrical tip clearances on cavitation performance and radial force of a mixed flow pump as turbine at pump mode, Renew. Energy 127 (2018) 368–376.

[80] A.P. Georgakakos, The value of streamflow forecasting in reservoir operation, JAWRA J. Am. Water Res. Assoc. 25 (4) (1989) 789–800.

[81] S.A. Wasimi, P.K. Kitanidis, Real-time forecasting and daily operation of a multireservoir system during floods by linear quadratic Gaussian control, Water Resour. Res. 19 (6) (1983) 1511–1522, https://doi.org/10.1029/WR019i006p01511.

[82] R. Krzysztofowicz, The case for probabilistic forecasting in hydrology, J. Hydrol. 249 (1–4) (2001) 2–9.

[83] H.R. Maier, A. Jain, G.C. Dandy, K.P. Sudheer, Methods used for the development of neural networks for the prediction of water resource variables in river systems: current status and future directions, Environ. Model. Softw 25 (2010) 891–909.

[84] A.Y. Shamseldin, Application of neural network technique to rainfall-runoff modelling, J. Hydrol. 199 (3–4) (1997) 272–294.

[85] S.K. Ahmad, F. Hossain, A globally scalable data-driven technique for forecasting of reservoir inflow for hydropower maximization, Environ. Model. Softw.**119**, (2019, 147-165. https://doi.org/10.1016/j.envsoft.2019.06.008)